



Contents lists available at ScienceDirect

Bioorganic & Medicinal Chemistry Letters

journal homepage: www.elsevier.com/locate/bmcl

Novel and highly potent histamine H3 receptor ligands. Part 1: withdrawing of hERG activity

Nicolas Levoïn*, Olivier Labeeuw, Thierry Calmels, Olivia Poupardin-Olivier, Isabelle Berrebi-Bertrand, Jeanne-Marie Lecomte, Jean-Charles Schwartz, Marc Capet

Bioprojet-Biotech, 4 rue du Chesnay Beauregard, BP 96205, 35762 Saint Grégoire, France

ARTICLE INFO

Article history:

Received 21 June 2011

Revised 4 July 2011

Accepted 5 July 2011

Available online 13 July 2011

Dedicated to Pr. Walter Schunack, in memoriam

Keywords:

Histamine

H3R

hERG

QSAR

ABSTRACT

Pre-clinical investigation of some aryl-piperidinyl ether histamine H3 receptor antagonists revealed a strong hERG binding. To overcome this issue, we have developed a QSAR model specially dedicated to H3 receptor ligands. This model was designed to be directly applicable in medicinal chemistry with no need of molecular modeling. The resulting recursive partitioning trees are robust (80–85% accuracy), but also simple and comprehensible. A novel promising lead emerged from our work and the structure–activity relationships are presented.

© 2011 Elsevier Ltd. All rights reserved.

Histamine H3 receptors (H3Rs) are widely distributed in the central nervous system where they modulate transmitter release, particularly in brain regions critical for cognition and sleep regulation. They are located presynaptically and postsynaptically, acting both as auto- and heteroreceptors. As autoreceptors, H3R negatively regulate the synthesis and release of histamine (negative feedback mechanism of histamine neurotransmission). As heteroreceptors, H3R modulate other neurotransmitters, through cholinergic, adrenergic, dopaminergic and serotonergic pathways.¹ Due to the effect of H3R signalling on multiple neuronal transmitters, H3R antagonists represent very promising drug candidates for the treatment of many CNS disorders, such as Alzheimer's disease, attention deficit hyperactivity disorder, schizophrenia, sleep dysfunctions and memory impairment.^{2–4} H3R ligands may also be useful in the control of pain.⁵

Our past work targeting H3R gave rise to many potent chemical series.^{6–9} From these medicinal chemistry efforts, FUB2.922 (Table 3) emerged as a very interesting lead, combining the advantages of displaying a strong H3R affinity ($K_i = 3$ nM) and being easily synthesizable. However, it turned out to have cardiovascular safety concerns. In particular, its strong inhibition of hERG channel (70% inhibition at 1 μ M), precluded it from being clinically developed.

To help and rationalize the chemical modifications that decrease hERG affinity, we built different models by use of published structure–activity relationships.

An ideal model in medicinal chemistry should be accurate, but also comprehensible and simple to interpret. So we turned towards ligand-based approaches. Many hERG models have been described in the literature,^{10–12} but, to our knowledge, none deals specifically with H3R ligands. This renders the applicability of existing pharmacophore and QSAR models questionable. Actually, these methods are known to be robust with their parent data, but to quickly loose their efficacy when chemical series diverge.^{13,14} To overcome this inherent limit, we used only H3R ligands to build a QSAR model for hERG activity, compiling recent data.¹⁵

We used 2D descriptors to alleviate conformational problems,¹⁶ and we chose recursive partitioning (RP) methodology because of its intuitive meaning. In a medicinal chemistry perspective, RP is actually amenable to visual and logical perception, and seems preferable to complex equations and mathematical models. The activity threshold was set to 7 μ M for hERG IC_{50} , dividing the dataset between 112 active and 105 inactive ligands. We obtained 2 RP models, of high statistical quality (Fig. 1).

The first tree contains 8 nodes and uses 8 descriptors.¹⁷ Nodes of the trees are globally pure (mean of 81%), and the worst node is 62% pure (Table 1). This tree is a very robust categorization tool since an accuracy of 86% was calculated.¹⁸ The second model is slightly less robust (accuracy of 81%), but has the advantage of

* Corresponding author.

E-mail address: n.levoïn@bioprojet.com (N. Levoïn).

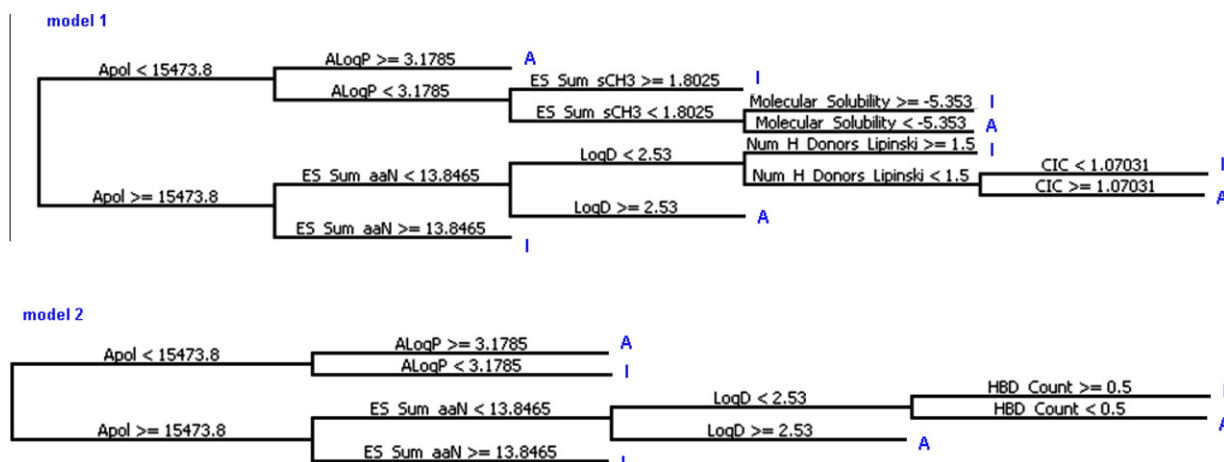


Fig. 1. The 2 RP models obtained with the training set (217 H3R ligands with hERG IC₅₀ ranging from 4 nM to 300 μM).¹⁵ 'A' means that the branch is mainly composed of active ligands (high hERG affinity). 'I' stands for mainly inactive molecules. The threshold was set to 7 μM. The meaning of descriptors abbreviation is given in.¹⁷

Table 1
Descriptive parameters of the 2 RP models

	Nodes	Descriptors	Tree depth	Mean purity	Worst purity	Accuracy	Sensitivity	Specificity
Model 1	8	8	5	0.81	0.62	0.86	0.88	0.83
Model 2	5	5	4	80	68	0.81	0.83	0.79

Table 2
Examples of simple chemical modifications of different scaffolds withdrawing hERG activity. References are given in [Supplementary data](#)¹⁵

Molecule	Fragment	HERG IC ₅₀ (μM)	ES Sum aaN	HBD Count	Apol	SI reference
EX1		0.1	13.7		16,496	5
EX2		23	17.5		15,331	5
EX3		1.9		0	17,980	10
EX4		7		1	16,953	10
EX5		3.7		0	12,295	1
EX6		40		1	11,900	1

being more interpretable than the precedent, because it is shorter and does not use topological descriptor (as CIC for the first RP). A reading of the RP tree is the following: if a molecule has descriptor $\text{Apol} < 15473.8$ and $\text{AlogP} \geq 3.1785$, then it might have hERG IC₅₀ < 7 μM (model 1). From a drug design perspective, the tree is a rational way of ameliorating the selectivity of H3R ligands. For in-

stance, a pyridinylthiazolopyridine is hERG active (see fragment of H3 ligand EX1 in [Table 2](#)).¹⁵ It has 3 aromatic nitrogens and sum aaN < 13.8465. Replacing pyridinyl by pyrimidinyl (increase in sum aaN in model 2) reduce greatly hERG binding (EX2). As another example, an ether derivative is hERG active (EX3). Adding a hydrogen-bond donor (HBD count in model 2) alleviates hERG is-

Table 3
New derivatives of FUB2 922, with variations of the phenyl A substituent. H3R^S : competition with [¹²⁵I]-iodoproxifan binding, hERG^S : competition with [³H]-Dofetilide binding

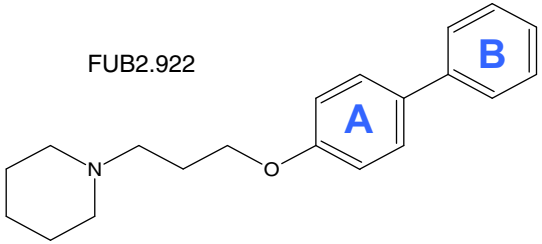
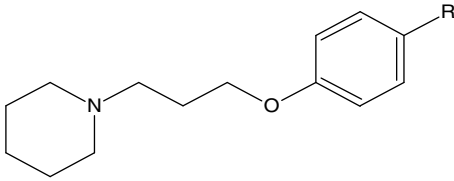
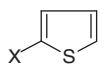
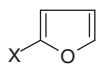
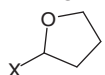
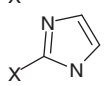
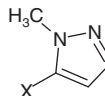
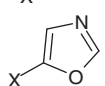
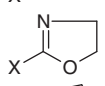
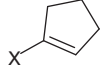
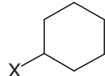
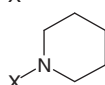
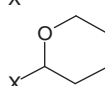
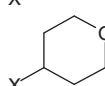
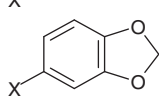
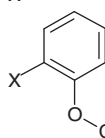
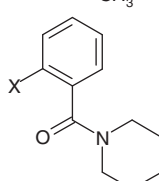
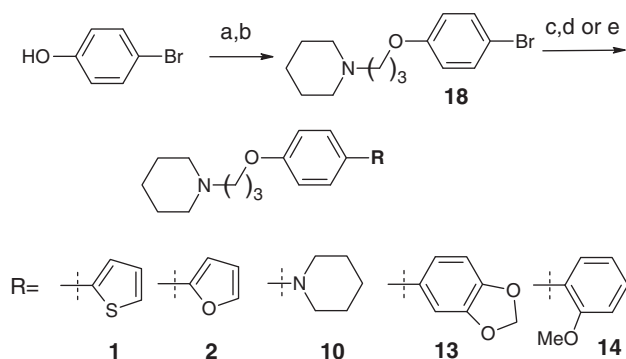
<div style="display: flex; justify-content: space-around; align-items: center;"> <div style="text-align: center;">  <p>FUB2.922</p> </div> <div style="text-align: center;">  </div> </div>								
Compound	R	Human recombinant		Apol	A log <i>P</i>	sum aaN	Log <i>D</i>	HBD Count
		H3R ^S Ki (nM)	hERG ^S Ki (nM)					
1		1.4	14	12993.4	4.4	0.0	2.8	0
2		5.0	90	11653.2	3.8	0.0	2.3	0
3		9.0	2747	11024.0	3.2	0.0	1.7	0
4		4.8	10,000	11434.0	2.7	4.2	1.6	1
5		1.8	190	11947.3	3.4	8.2	1.8	0
6		2.5	1194	11345.6	2.6	3.9	1.1	0
7		3.6	10,000	11030.9	2.9	0.0	1.3	0
8		1.6	230	11507.1	4.4	0.0	2.9	0
9		2.8	13	11705.7	5.1	0.0	3.6	0
10		4.9	841	11625.7	4.0	0.0	1.7	0
11		5.2	1125	11537.2	3.7	0.0	2.1	0
12		8.3	2220	11537.2	3.4	0.0	1.8	0
13		3.6	5	13711.7	4.2	0.0	2.7	0
14		2.2	76	13507.7	4.4	0.0	2.9	0
15		1.6	818	16475.8	4.8	0.0	3.2	0

Table 3 (continued)

Compound	R	Human recombinant		Apol	A log P	sum aaN	Log D	HBD Count
		H3R ^S Ki (nM)	hERG ^S Ki (nM)					
16		10.4	8	14988.3	4.7	0.0	3.1	0
17		0.2	10,000	13165.5	4.6	0.0	1.4	0



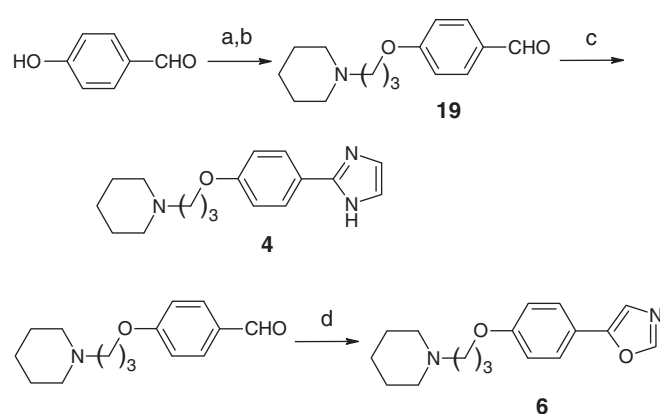
Scheme 1. Synthesis of compounds **1**, **2**, **10**, **13** and **14**. Reagents and conditions: (a) 1-bromo-3-chloropropane, K₂CO₃, DMF, rt, 15 h; (b) piperidine, K₂CO₃, KI, DMF, 100 °C, 15 h; (c) 2-thiopheneboronic acid (for **1**) or 3,4-methylenedioxyphenylboronic acid (for **13**) or 2-methoxyphenylboronic acid (for **14**), Pd(PPh₃)₄, toluene or THF, 100 °C, 15 h; (d) 2-(tributylstannyl)furan, PdCl₂(PPh₃)₂, THF, reflux, 15 h; (e) piperidine, tBuONa, Pd₂(dba)₃, BINAP, toluene, 100 °C, 15 h.

sue (hydroxyl in EX4). Butenone to amide isosterism is another illustration (EX5/EX6).

For both trees, the most differentiating nodes deal with lipophilic character of the molecules (Apol, A log P, log D),¹⁷ as well as aromatic tendency (aaN). This reflects most important aspects for hERG affinity, at least for H3 ligands. Hence, modulating lipophilicity of our lead FUB2.922 (Table 3) should have strong effect in its hERG profile.

We tested this hypothesis by varying the phenyl A substituents (Table 3). The synthetic route for the compounds reported herein is illustrated in Schemes 1–7.

The first compounds (Scheme 1) were synthesized by palladium-catalyzed cross-coupling reactions of aryl bromide intermediate **18** with aryl- or heteroarylboronic acids (compounds **1**, **13**



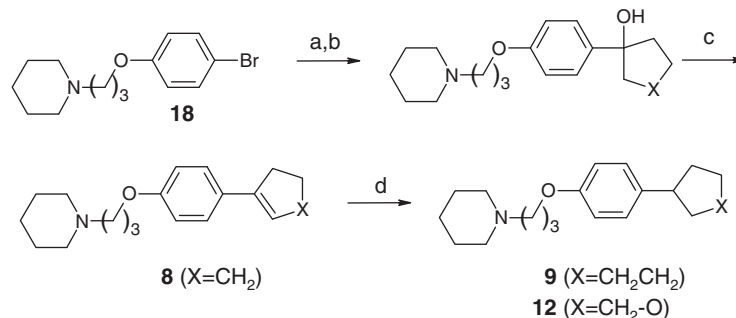
Scheme 3. Synthesis of compounds **4** and **6**. Reagents and conditions: (a) 1-bromo-3-chloropropane, K₂CO₃, DMF, rt, 15 h; (b) piperidine, K₂CO₃, KI, DMF, 110 °C, 3 h; (c) glyoxal, NH₄OH, EtOH/H₂O, rt, 15 h; (d) TosMIC, MeOH, K₂CO₃, reflux, 2 h.

and **14**), 2-(tributylstannyl)furan (compound **2**) or piperidine (compound **10**). Compound **18** was obtained from commercially available 4-bromophenol after condensation with 1-bromo-3-chloropropane and piperidine.

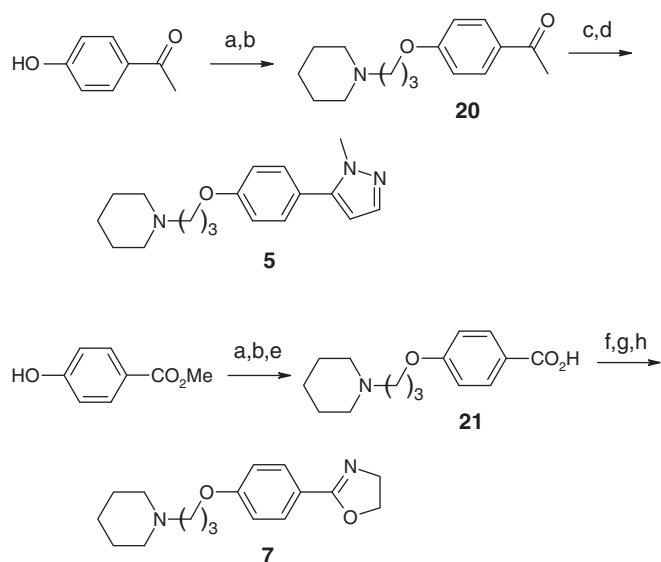
The common intermediate **18** was also used to form the corresponding Grignard or lithium reagents. Condensation with cycloalkylketones or tetrahydropyran-4-one, dehydration and subsequent hydrogenation allowed to access to **8**, **9** and **12**.

Imidazole **4** and oxazole **6** were synthesized as shown in scheme 3 from benzaldehyde **19**, readily accessible from 4-hydroxybenzaldehyde. Pyrazole **5** and oxazoline **7** were prepared from the corresponding acetophenone **20** or carboxylic acid **21** (scheme 4).

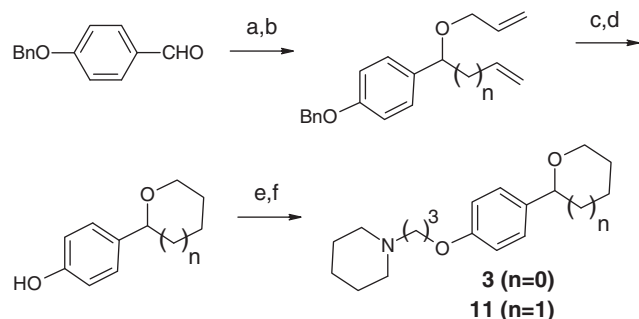
The synthesis of the tetrahydrofuran or -pyran moieties in **3** and **11** required a RCM (ring closure metathesis) strategy employing adequate vinyl or allyl derivatives (scheme 5).



Scheme 2. Synthesis of compounds **8**, **9** and **12**. Reagents and conditions: (a) Mg, THF or BuLi, THF –78 °C to 0 °C, 1 h; (b) cyclopentanone (for **8**) or cyclohexanone (for **9**) or tetrahydropyran-4-one (for **12**), THF, 0 °C, 2 h; (c) H₂SO₄, EtOH, rt, 2 h; (d) 1 atm H₂, 5% Pd/C, EtOH, rt 15 h.



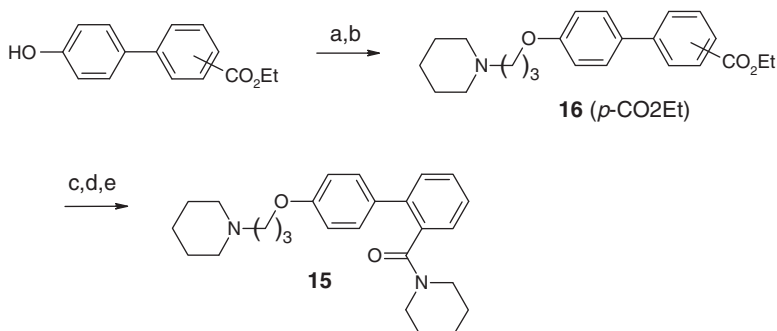
Scheme 4. Synthesis of **5** and **7**. Reagents and conditions: (a) 1-bromo-3-chloropropane, K_2CO_3 , DMF, rt, 15 h; (b) piperidine, K_2CO_3 , KI, DMF, 80 °C, 6 h; (c) NaH, THF, then HCO_2Me , rt, 2.5 h; (d) $MeNH-NH_2$, THF, rt, 1 h; (e) NaOH, MeOH, reflux, 30 min; (f) $SOCl_2$, rt, 15 h; (g) 2-chloroethylamine, NEt_3 , $CHCl_3$, rt, 7 h; (h) DBU, DCM, reflux, 24 h.



Scheme 5. Synthesis of compounds **3** and **11**. Reagents and conditions: (a) vinylmagnesium bromide (for **3**) or allylmagnesium bromide (for **11**), THF, THF, 40 °C, 15 min; (b) NaH, DMF, then allyl bromide, rt, 1 h; (c) Grubbs' catalyst 2nd generation, CH_2Cl_2 , reflux, 24 h; (d) 3 bar H_2 , 10% Pd/C, EtOH, rt, 15 h; (e) 1-bromo-3-chloropropane, K_2CO_3 , DMF, rt, 20 h; (f) piperidine, K_2CO_3 , KI, DMF, 60 °C, 5 h.

Preparation of compounds **16** and **15** relied on the usual introduction of the side chain by alkylation of phenols and the transformation of an ester into an amide function (scheme 6).

The desired dimethylcyclohexylamine **17** was prepared via a reductive amination reaction of cyclohexanone **22** (scheme 7).



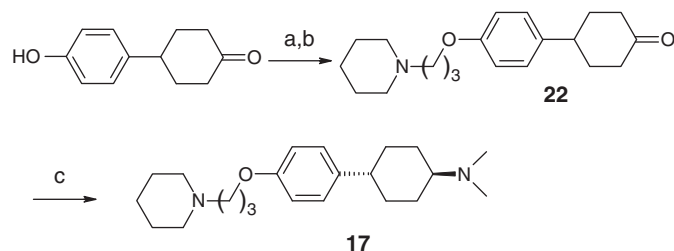
Scheme 6. Synthesis of compounds **15** and **16**. Reagents and conditions: (a) 1-bromo-3-chloropropane, K_2CO_3 , CH_3CN , reflux, 18 h; (b) piperidine, K_2CO_3 , KI, CH_3CN , reflux, 15 h; (c) NaOH, EtOH, reflux, 3 h; (d) $(COCl)_2$, DCM, DMF, rt, 1 h; (e) piperidine, rt, 1 h.

The *trans* isomer was purified by careful flash chromatography over silica.

Reducing the aromaticity appears as a general solution to decrease hERG binding (see furan **2** and tetrahydrofuran **3**, oxazoline **6** and oxazole **7**), but some heterocycle isosters also permit the reduction of hERG affinity (oxazoles vs furan or thiophene). By combining heteroatom introduction and hydrophobicity reduction, hERG binding can be largely abrogated (imidazole **4**). Even with aliphatic groups, introducing heteroatoms greatly diminishes hERG affinity (compare cyclohexyl **9** vs piperidine **10** or tetrahydropyrans **11** and **12**). Thus, the derivatives presented here clearly show the importance of lipophilicity and polarity of the molecules. In the extreme, the addition of a formal charge is another solution to attenuate hERG issue: compound **17** is the lowest binder for hERG, though being the most potent H3R ligand of the series presented here.

For our QSAR models, these variations constitute an external dataset to test the predictive behavior of our QSAR models. Table 4 shows that model 1 and 2 predict rather correctly the hERG class of the new molecules (89% accuracy), even if they are less specific than for the training set (67% vs 79% or 83%).

We have previously described a structure-based approach to deal with hERG issue, using a refined docking/scoring protocol.¹⁹ We confronted this homology model to the current datasets of H3R ligands. We obtained an accuracy of 73% for the training set, and 65% for the test set using a customized Ludi_2 scoring function. This suggests that structure-base approach is less precise than the RP models presented here, but on the other hand, docking is



Scheme 7. Synthesis of compound **17**. Reagents and conditions: (a) 1-bromo-3-chloropropane, K_2CO_3 , DMF, rt, 15 h; (b) piperidine, K_2CO_3 , KI, DMF, 80 °C, 6 h; (c) Me_2NH , $NaBH(OAc)_3$, AcOH, THF, rt, 15 h.

Table 4

Statistical analysis of the 2 RP models with the test set

	Accuracy	Sensitivity	Specificity
Model 1	0.89	0.93	0.67
Model 2	0.89	0.93	0.67

much more informative in terms of structural information. So the gold-standard should combine both approaches.

Our past drug discovery efforts in the H3R resulted in the very interesting lead FUB2.922. However, it had not been developed due to its high hERG affinity. To overcome this issue, we build a QSAR tool specially dedicated to H3R ligands. We chose a model that is easily understandable and useful for the non-specialist in molecular modeling, that is, RP. The trees presented in Fig. 1 are thus practically interpretable, and might be very useful for medicinal chemists involved in H3 area. They are statistically very robust, as judged by the accuracy calculated from the training set. An external test set constituted of close analogs of FUB2.922 demonstrate their predictive capacity.

Variation of the lipophilicity of the biphenyl had clearly shown a strong influence on hERG affinity, as revealed by the structure–activity relationships presented here. This brings to compound 17, the lead of a new chemical series described in the companion paper.²⁰

Acknowledgments

We thank Isabelle Delimoge, Marie-Noëlle Legave, Stéphanie Le Meur, Philippe Guibet, Benoît Messenger, and Sébastien Nicolas for their expert technical assistance.

Supplementary data

Supplementary data associated with this article can be found, in the online version, at doi:10.1016/j.bmcl.2011.07.006.

References and notes

- Brioni, J. D.; Esbenshade, T.; Garrison, T.; Bitner, S.; Cowart, M. J. *Pharmacol. Exp. Ther.* doi: 10.1124/jpet.110.166876.
- Leurs, R.; Bakker, R. A.; Timmerman, H.; de Esch, I. J. P. *Nat. Rev. Drug Discov.* **2005**, *4*, 107.
- Esbenshade, T. A.; Fox, G. B.; Cowart, M. D. *Mol. Interventions* **2006**, *6*, 77.
- Sander, K.; Kottke, T.; Stark, H. *Biol. Pharm. Bull.* **2008**, *31*, 2163.
- Hough, L.; Rice, F. L. *J. Pharmacol. Exp. Ther.* doi: 10.1124/jpet.110.171264.
- Ganellin, C. R.; Leurquin, F.; Piripitsi, A.; Arrang, J.-M.; Garbarg, M.; Ligneau, X.; Schunack, W.; Schwartz, J.-C. *Arch. Pharm. Pharm. Med. Chem.* **1998**, *331*, 395.
- Meier, G.; Ligneau, X.; Pertz, H. H.; Ganellin, C. R.; Schwartz, J.-C.; Schunack, W.; Stark, H. *Bioorg. Med. Chem.* **2002**, *10*, 2535.
- Lazewska, D.; Ligneau, X.; Schwartz, J.-C.; Schunack, W.; Stark, H.; Kiec-Kononowicz, K. *Bioorg. Med. Chem.* **2006**, *14*, 3522.
- von Coburg, Y.; Kottke, T.; Weizel, L.; Ligneau, X.; Stark, H. *Bioorg. Med. Chem. Lett.* **2009**, *19*, 538.
- Thai, K.-M.; Ecker, G. F. *Bioorg. Med. Chem.* **2008**, *16*, 4107.
- Su, B.-H.; Shen, M.-Y.; Esposito, E. X.; Hopfinger, A. J.; Tseng, Y. J. *J. Chem. Inf. Model.* **2010**, *50*, 1304.
- Johnson, S. R.; Yue, H.; Conder, M. L.; Shi, H.; Doweiko, A. M.; Lloyd, J.; Levesque, P. *Bioorg. Med. Chem.* **2007**, *15*, 6182.
- Kühne, R.; Ebert, R.-U.; Schüürmann, G. J. *Chem. Inf. Model.* **2006**, *46*, 636.
- Hansen, K.; Rathke, F.; Schroeter, T.; Rast, G.; Fox, T.; Kriegl, J. M.; Mika, S. J. *Chem. Inf. Model.* **2009**, *49*, 1486.
- Supplementary data
- Ermondi, G.; Visentin, S.; Caron, G. *Eur. J. Med. Chem.* **2009**, *44*, 1926.
- All the descriptors are available in Discovery Studio or Pipeline Pilot (Accelrys, San Diego, CA). **Apol** is the sum of atomic polarizabilities, **A log P** is the log of octanol–water partition calculated coefficient, **Log D** is the same partition coefficient taking into account the ionization state of the molecule, **molecular solubility** is the log of calculated solubility (in mol/L), and **HBD Count** is the sum of hydrogen-bond donor functions. **sum aaN** is the electrotopological state sum of aromatic nitrogens (Hall L., Kier L., *J. Chem. Inf. Comput. Sci.* **2000**, *40*, 784–791.). **CIC** is a graph-theoretical topological descriptor (Bonchev, D., *Information Theoretic Indices for Characterization of Chemical Structures, Chemometrics Series*, ed. D.D. Bawden, **1983**, *5*, New York: Research Studies Press Ltd.). There is almost a correlation between sum_aaN and the number of aromatic nitrogens, so a simple estimate of sum aaN may be the following: **sum_aaN** = 0.24 + (4.37 * number of aromatic nitrogens). As an approximation, we can consider that **Apol** exceed the threshold of 15473.8 if one of the above conditions is established: (i) either the molecule contains 10 or more double-bonds, (ii) or the molecule contains 8 or more double-bonds and 1 or more halogen, sulfur, phenolic oxygen or aniline nitrogen
- Quality of the models is evaluated by their accuracy, sensitivity and specificity, as follow:

$$\text{Accuracy} = \frac{\text{TP} + \text{TN}}{\text{TP} + \text{TN} + \text{FP} + \text{FN}}, \text{Sensitivity} = \frac{\text{TP}}{\text{TP} + \text{FN}}, \text{Specificity} = \frac{\text{TN}}{\text{TN} + \text{FP}}$$

true positives (TP) and true negatives (TN) are hERG binders or not binders at a 7 μM threshold, correctly classified by the model. False negatives (FN) and false positives (FP) are hERG binders or not binder misclassified.
- Levoine, N.; Calmels, T.; Poupardin-Olivier, O.; Labeeuw, O.; Danvy, D.; Robert, P.; Berrebi-Bertrand, I.; Ganellin, C. R.; Schunack, W.; Stark, H.; Capet, M. *Arch. Pharm. Pharm. Med. Chem.* **2008**, *341*, 610.
- Labeeuw, O.; Levoine, N.; Poupardin-Olivier, O.; Calmels, T.; Ligneau, X.; Berrebi-Bertrand, I.; Robert P.; Lecomte, J.-M.; Schwartz, J.-C.; Capet, M. *Bioorg. Med. Chem. Lett.* doi:10.1016/j.bmcl.2011.06.102.